Published in final edited form as:
Structure. 2009 July 15; 17(7): 974–980. doi:10.1016/j.str.2009.04.011.

Replication across template T/U by human DNA polymerase-ι

Rinku Jain[1], **Deepak T. Nair**[1,2], **Robert E. Johnson**[3], **Louise Prakash**[3], **Satya Prakash**[3], and **Aneel K. Aggarwal**[1]

[1]Department of Structural and Chemical Biology, Mount Sinai School of Medicine, Box 1677, 1425 Madison Avenue, New York, NY 10029

[2]National Centre for Biological Sciences (NCBS-TIFR), UAS-GKVK Campus, Ballary Road, Bangalore 560065, India

[3]Department of Biochemistry and Molecular Biology, 301 University Blvd., University of Texas Medical Branch, Galveston, TX 77755-1061

Summary

Human DNA polymerase-ι (Polι) incorporates correct nucleotides opposite template purines with a much higher efficiency and fidelity than opposite template pyrimidines. In fact, the fidelity opposite template T is so poor that Polι inserts an incorrect dGTP approximately 10 times better than it inserts the correct dATP. We determine here how a template T/U is accommodated in the Polι active site and why a G is incorporated more efficiently than an A. We show that in the absence of incoming dATP or dGTP (binary complex), template T/U exists in both *syn* and *anti* conformations, but in the presence of dATP or dGTP (ternary complexes), template T/U is predominantly in the *anti* conformation. We also show that dATP and dGTP insert differently opposite template T/U, and that the basis of selection of dGTP over dATP is a hydrogen bond between the N2 amino group of dGTP and Gln59 of Polι.

Introduction

The survival of organisms depends critically on the ability to faithfully replicate DNA. As such, virtually all DNA polymerases replicate DNA by incorporating the nucleotide that forms the correct Watson-Crick base pair with the template base. In addition, the catalytic efficiencies with which any given polymerase forms the four possible correct base pairs are approximately the same, reflecting the near geometric identities of Watson-Crick, A.T, T.A, G.C, and C.G base pairs. This basic tenet holds for high fidelity replicative DNA polymerases and is also generally valid for the lower fidelity Y family DNA polymerases that possess the ability to replicate through DNA lesions (Prakash et al., 2005). Human DNA polymerase ι (Polι), a member of the Y family of DNA polymerases, is a notable exception to these rules. Polι incorporates nucleotides opposite template purines with a much higher efficiency and fidelity than opposite template pyrimidines. Specifically, Polι exhibits the highest efficiency and fidelity opposite template A, followed by template G, and then templates C and T. In fact, the fidelity opposite template T is so poor that Polι inserts an incorrect dGTP approximately 10 times better than it inserts the correct dATP (Haracska et

*Correspondence: aneel.aggarwal@mssm.edu.

al., 2001; Johnson et al., 2000; Tissier et al., 2000; Washington et al., 2004; Zhang et al., 2000).

The ternary crystal structures of Polι bound to template purines and the correct incoming dNTP have yielded major insights into the action mechanism of this polymerase. Specifically, in the structure of Polι bound to template A and an incoming dTTP, the templating A adopts a *syn* conformation and forms a Hoogsteen base pair with the incoming T, which remains in the *anti* conformation (Nair et al., 2006b; Nair et al., 2004). Similarly, in the structure of Polι paired with a template G and an incoming dCTP, a G.C+ Hoogsteen base pair is formed in the polymerase active site (Nair et al., 2005; Nair et al., 2006b). Hoogsteen base pairing provides a basis for the much higher efficiency and fidelity of nucleotide incorporation opposite template purines than opposite pyrimidines because only the templates A and G have a Hoogsteen edge by which they can establish two hydrogen bonds with the correct incoming pyrimidine nucleotide. The ability to form Hoogsteen base pairs allows Polι to promote replication through adducts such as 1, N6-ethenodeoxyadenosine that disrupt the Watson-Crick (W-C) edge but not the Hoogsteen edge of the templating purine (Nair et al., 2006a).

Compared to the purine templates, Polι is highly inefficient at incorporating the correct nucleotide A opposite template T; moreover, it incorporates a G opposite template T with an ~ 10-fold better catalytic efficiency than an A (Haracska et al., 2001; Johnson et al., 2000; Tissier et al., 2000; Washington et al., 2004; Zhang et al., 2000). However, even the incorporation of G opposite template T occurs almost 100-fold less efficiently than, for example, the incorporation of T opposite template A. We determine here how a template T is accommodated in the Polι active site and why G is incorporated more efficiently than an A. We show that in the absence of dATP or dGTP (binary complex), template T exists in both *syn* and *anti* conformations, but in the presence of dATP or dGTP (ternary complexes), template T is predominantly in the *anti* conformation. We also show that dATP and dGTP insert differently opposite template T, and that the basis of selection of dGTP over dATP is a hydrogen bond between the N2 amino group of dGTP and Gln59 of Polι.

Results

Structure determination

We crystallized Polι with “double-ended” 18-nt template-primers designed to present template T in the active sites of two symmetrically bound Polι molecules (see Methods). We have used a similar strategy previously to crystallize Polι with undamaged and damaged DNAs (Nair et al., 2005; Nair et al., 2006a; Nair et al., 2006b; Nair et al., 2009). Cocrystals in the absence (binary) and presence of incoming dATP and dGTP (ternary) were obtained under identical conditions (from PEG solutions), belonging to space group $P6_522$ with cell dimensions of a = 98 Å, b = 98 Å, c = 203Å and α=β=90°, γ=120°. The $Polι_T$, $Polι_{T.dATP}$ and $Polι_{T.dGTP}$ structures were solved by molecular replacement (MR) using the structure of the $Polι_{G.dCTP}$ complex (with dCTP omitted) as a search model (Nair et al., 2005). However, in all three structures, electron densities for the template T were not as well-defined as for the template purines in previous Polι structures (Nair et al., 2005; Nair et al., 2006a; Nair et al., 2006b; Nair et al., 2004). To help fix the conformation(s) of the thymines, we substituted 5-bromouracil (BrU) for thymine in the template-primers and cocrystallized them with Polι in the absence and presence of incoming dATP and dGTP. We solved the $Polι_U$, $Polι_{U.dATP}$ and $Polι_{U.dGTP}$ structures by MR and the resulting electron density maps were very similar to those obtained for the $Polι_T$, $Polι_{T.dATP}$ and $Polι_{T.dGTP}$ complexes. However, the anomalous signal of the Br atoms permitted the calculation of anomalous difference Fourier maps, which pinpointed the positions of the Br atoms and showed that BrU (and T, by analogy) exists in both *syn* and *anti* conformations in the binary $Polι_U$ complex, but switches

primarily to the *anti* conformation in the Polι$_{U.dATP}$ and Polι$_{U.dGTP}$ ternary complexes. The Polι$_{U}$, Polι$_{U.dATP}$ and Polι$_{U.dGTP}$ complexes were selected for further refinement to 2.3Å, 2.85Å, and 2.2Å resolutions (Table 1), respectively, with the BrUs in alternate *anti:syn* conformations in 0.5:0.5, 0.9:0.1, and 0.7:0.3 ratios, respectively. The refined Polι$_{U}$ binary complex (R_{free} of 28.0%; R_{crys} of 25.2%) contains Polι residues 26-370, 379-394 and 404-414 (the first 25 and the last 6 residues are disordered, and residues 371-378 and 395-403 comprising two loops in the PAD have poor density), DNA nucleotides 3-11 (two of the four unpaired template nucleotides at the 5' end are disordered), and 237 water molecules. The refined Polι$_{U.dATP}$ ternary complex (R_{free} of 28.2%; R_{crys} of 24.1 %) contains Polι residues 25-370, 379-394 and 404-414, DNA nucleotides 3-11, incoming dATP, 1 Mg^{2+} ion, and 156 water molecules. The refined Polι$_{U.dGTP}$ ternary complex (R_{free} of 27.0%; R_{crys} of 25.4%) contains Polι residues 25-370, 379-394 and 404-414, DNA nucleotides 3-11, incoming dATP, 2 Mg^{2+} ions, and 272 water molecules. All three structures have good stereochemistry, with ~86% of the residues in the most favored regions of the Ramachandran plot and <0.3% in the disallowed regions for Polι$_{U.}$ and Polι$_{U.dGTP}$, and ~ 83% in the most favored region and < 0.6% in the disallowed region for Polι$_{U.dATP}$.

Overall arrangement

In all three complexes, a Polι molecule binds to each end of the double-ended template primer (Fig. 1). The two molecules are related by a crystallographic two-fold axis and thus make identical contacts with the template-primer. Polι has the familiar right-handed architecture with palm (residues 25-37, 99-224), fingers (38-98), and thumb (225-288) domains, and the PAD (polymerase associated domain; residues 298-414) unique to Y-family polymerases (Fig.1). The palm forms the floor of the DNA binding cavity and carries the active site residues (Asp34, Asp126 and Glu127), while the fingers domain lies over the templating base (and the incoming nucleotide in the ternary complexes). The thumb and the PAD are connected by a long linker that spans the width of the DNA. The thumb skims the minor groove surface on one side the template-primer, while the PAD docks in the major groove on the other side (Fig. 1). The interface between the two Polι molecules is relatively small, with ~700 $Å^2$ of surface area buried between the thumb domain of one polymerase and the PAD of the other. The majority of Polι-DNA interactions are mediated by the PAD, wherein the main chain amides on "outer" β-strands of the PAD β-sheet make a series of hydrogen bonds with the template and primer strands.

The Polι$_{U}$ binary complex

The palm, fingers and thumb domains and the PAD occupy identical positions with respect to the template-primer as in previous Polι structures (Nair et al., 2005; Nair et al., 2006a; Nair et al., 2006b; Nair et al., 2004), and the Polι$_{U.dATP}$ and Polι$_{U.dGTP}$ ternary complexes described below. Thus, there is no open or closed form of Polι analogous to replicative DNA polymerases, wherein the fingers domain rotates by as much as ~40° in response to dNTP binding (Doublie et al., 1999; Rothwell and Waksman, 2005). The major difference between Polι$_{U}$ and the Polι$_{A}$ and Polι$_{G}$ binary complexes determined previously is in the DNA (Nair et al., 2006b). In the Polι$_{A}$ and Polι$_{G}$ binary complexes, the purines are in the *anti* conformation, which flip to the *syn* conformation in reaction to dNTP binding (Nair et al., 2006b). Once in the *syn* conformation, the Hoogsteen edge of A and G is available for hydrogen bonding with the W-C edge of incoming dTTP and dCTP, respectively. In contrast, in the Polι$_{U}$ binary complex, template U adopts a mixture of *anti* and *syn* conformations (Fig. 2). In response to dATP or dGTP binding (described below), occupancy for the *anti* conformation increases while that for the *syn* conformation decreases. Unlike purines, pyrimidines lack a Hoogsteen edge. Thus, it is only in the *anti* conformation that the polar atoms on T/U (N3, O2, and O4) are available for hydrogen bonding with dATP or dGTP in the Polι active site.

The Polι$_{U.dATP}$ ternary complex

In the Polι$_{A.dTTP}$ and Polι$_{G.dCTP}$ ternary complexes, incoming dNTP effectively pushes the templates A and G into the *syn* conformation for if they were to remain in *anti* conformation they would clash with the incoming nucleotide (Nair et al., 2005; Nair et al., 2006b; Nair et al., 2004). By contrast, in the Polι$_{U.dATP}$ ternary complex (and the Polι$_{U.dGTP}$ complex – described below), it is the *syn* rather than the *anti* conformation of the template base that clashes with the incoming nucleotide, wherein the C5 Br (or CH3 in the case of T) sterically overlaps with the W-C edge of incoming dNTP (Fig. 3). The small fraction of template T in the *syn* conformation in the ternary complex crystals likely reflects a fraction of complexes without incoming dNTP in the binary state. In the description below, we refer mainly to the *anti* conformation.

To account for the poor efficiency of Polι in inserting A opposite template T, we had considered a model in which the template T/U is evicted from the active site and dATP is inserted opposite an essentially “abasic” site. This is clearly not the case. The structure reveals unexpected *trans* U:A base pairing (Figs, 3A and B) (Leontis et al., 2002). By comparison to a standard Watson-Crick (WC) T/U:A base pair, where the glycosidic bonds of the two nucleosides are in *cis*, the U and A in our structure are in *trans* or antiparallel to one another. The C1’-C1’ distance is 11.2Å, as compared to ~10.5Å in a standard W-C base pair. Also, because the glycosidic angles of both U and A are *anti*, they couple with the trans orientation of the glycosidic bonds to produce local parallel-stranded DNA at the nascent base-pair (Leontis et al., 2002). In a standard *cis* T/U:A base pair, the N1 and N6 atoms of A form hydrogen bonds with the N3 and O4 atoms of T/U, respectively. In a *trans* T/U:A base pair, we can imagine A inverting around the N1(A)…N3(T) hydrogen bonds to generate a potential new N6(A)…O2(T/U) hydrogen bond in place of the N6(A)…4(T/U) hydrogen bond (Fig. 3). The N1(A)…N3(U) and N6(A)…O2(U) distances in our structure are 2.71Å and 3.52Å, respectively.

In all previous Polι ternary complexes, the incoming dNTP sugar packs against the aromatic ring of Tyr39 and a hydrogen bond is also made between its 3’OH and the main chain amide of the tyrosine (Nair et al., 2005; Nair et al., 2006a; Nair et al., 2006b; Nair et al., 2009; Nair et al., 2004). In the present structure, as the result of dATP inverting to the *trans* conformation, the sugar is removed from the aromatic ring of Tyr39 and is close to surface of the major groove. Although, the dATP triphosphate moiety lies between the palm and fingers domains as in previous Polι structures it weaves a different path (Fig. 3A). The α- and β-phosphates, for example, are displaced by >4Å from their positions in previous Polι structures, and as a consequence some interactions are lost while others are maintained. For example, Thr65 and Tyr68 on the fingers domain are unable to make hydrogen bonds with the β- and γ- phosphates, respectively, but Arg71 from the fingers domain and Lys214 from the palm domain are still able to reach and make bonds with the β- and γ- phosphates (Fig. 3A). Also, because of the displacement of the α-phosphate the active geometry is incompatible with catalysis, with the putative 3’OH at the primer terminus located >6Å from the α-phosphate of incoming dNTP.

The Polι$_{U.dGTP}$ ternary complex

In contrast to dATP, dGTP inserts in *cis* opposite template U (Fig. 3). The structure suggests distorted U:G base pairing in which the U is either ionized or exists as an enol tautomer (Lawley and Brookes, 1962;Sowers et al., 1987;Topal and Fresco, 1976;Watson and Crick, 1953). That is, the U and G bases lie opposite one another in distorted W-C geometry rather than the more common wobble geometry (Fig. 3). Although T/U occurs predominantly as a keto tautomer, it can also exist as a rare enol tautomer and in an ionized form that can pair with G via W-C geometry (Lawley and Brookes, 1962;Sowers et al., 1987;Topal and Fresco,

1976;Watson and Crick, 1953). In the structure, the N3 and O2 atoms of U make putative hydrogen bonds with the N1 atom and N2 amino group of G, respectively. The U and G bases are staggered and propeller twisted with respect to each other, and the hydrogen bond between O2(U) and N2(G) is relatively short (~2.45Å), which may be indicative of an ionized form of U (rather than the enol tautomer). Interestingly, BrU (used in our structural analysis) has a greater tendency than T/U to pair with G and this property has been ascribed to the increased propensity of BrU to form the enol tautomer or the ionized form (Danilov et al., 2009;Lawley and Brookes, 1962;Sowers et al., 1987). However, in crystal and NMR structures of DNAs containing BrUs (Brown et al., 1986;Sowers et al., 1989), BrU pairs with G in much the same way as unmodified U/T, namely via wobble geometry. Intriguingly, NMR spectra at high pH (9.8) (Sowers et al., 1989), suggests an ionized BrU;G W-C base pair with a geometry similar to what we observe here in the $Pol\iota_{U.dGTP}$ complex (crystallized at a pH of 6.5).

The incoming dGTP triphosphate moiety interleaves between the palm and fingers domains, and makes hydrogen bonds with Thr65, Tyr68, and Arg71 from the fingers domain, and Lys214 from the palm domain. The triphosphate moiety and the catalytic residues Asp34, Asp126 and Glu127 coordinate two putative Mg^{2+} ions in the active site. The geometry of the active site is better poised for catalysis than in the $Pol\iota_{U.dATP}$ structure, with the putative 3'OH at the primer terminus located ~3.3Å from the dGTP α-phosphate and aligned more or less linearly with respect to the scissile Pα O3' bond.

The C1'-C1' distance across the U:G base pair is ~9.6Å, as compared to ~10.5Å in a standard W-C base pair. In previous Polι structures with undamaged and damaged DNAs, the C1'-C1' distance across the nascent pairs ranges from ~8.5 to ~9.1Å, wherein the template sugar is entrenched in a cavity lined by residues from the fingers domain, including the side chain of Leu62 and the aliphatic portions of Gln59 and Lys60 (Nair et al., 2005; Nair et al., 2006a; Nair et al., 2006b; Nair et al., 2004). On the other side of the active site, the dNTP sugar is fixed by packing against the aromatic ring of Tyr39, as well as by a hydrogen bond between its 3'OH and the main chain amide of the tyrosine. The resulting constriction in C1'-C1' distance across the sugars is conducive to Hoogsteen base pairing opposite template purines (Nair et al., 2005; Nair et al., 2006b; Nair et al., 2004). In the present structure, a change in the Leu62 rotamer (from χ2 of 169° in $Pol\iota_{G.dCTP}$ to 116° $Pol\iota_{U.dGTP}$) allows the template U sugar to shift by ~1Å and still fit within the hydrophobic cavity delineated by Leu62, Gln59, Lys60. The most revealing feature of our structure is a hydrogen bond between the N2 amino group of incoming dGTP and OE1 of Gln59 (2.9Å) on the fingers domain (Figs. 3A and D). This direct hydrogen bond between G and the polymerase appears to be the key stabilizing interaction favoring the insertion of G over A opposite template T in the Polι active site. That is, even if incoming dATP was to assume a *cis* configuration with respect to template T/U it would be unable to make this hydrogen bond because it lacks an N2 amino group.

To evaluate the significance of the observed hydrogen bond between Gln59 and the N2 amino group of incoming dGTP, we compared the catalytic efficiencies (k_{cat}/K_m) of dGTP *vs*. dITP incorporation using steady-state kinetic analyses (Johnson et al., 2000; Nair et al., 2006a). Since dITP lacks the N2 amino group, any reduction in the efficiency of dITP incorporation would result from the contribution of hydrogen bonding between the N^2 amino group of dGTP and OE1 of Gln59 to dGTP incorporation. As shown in Table 2, compared to dGTP, dITP incorporation is reduced by 10-fold opposite template T. We infer from this observation that hydrogen bonding of Gln59 with the N2 amino group of dGTP contributes positively to G incorporation opposite template T and could account for the preferential incorporation of G over an A opposite template T.

Discussion

Compared to the purine templates, Polι is highly inefficient at incorporating the correct nucleotide A opposite template T. In fact, the fidelity opposite template T is so poor that Polι inserts an incorrect G roughly 10 times better than it inserts the correct A (Haracska et al., 2001; Johnson et al., 2000; Tissier et al., 2000; Washington et al., 2004; Zhang et al., 2000). However, even the incorporation of G opposite template T occurs almost 100-fold less efficiently than, for example, the incorporation of T opposite template A. Perhaps reflective of this inefficiency opposite template T, the electron density for template U/T (and incoming nucleotides in the ternary complexes) is not as well-defined as in Polι structures with template purines (Nair et al., 2005; Nair et al., 2006b; Nair et al., 2004). Nonetheless, via the use of bromouracils we have gained some insights into how a template U/T may be accommodated in the Polι active site and why a G is incorporated more efficiently than an A.

In the $Pol\iota_U$ binary complex, template U/T exists in both *syn* and *anti* conformations. In contrast, in the $Pol\iota_A$ and $Pol\iota_G$ binary complexes the purine is exclusively in the *anti* conformation (Nair et al., 2006b); which then flips over to the *syn* conformation in the presence of incoming dATP or dGTP (in ternary complexes). The existence of template U/T in *syn* conformation is somewhat surprising since pyrimidines are considered less likely than purines to adopt the *syn* conformation due to potential steric overlap between the O2 and the sugar atoms (Haschemeyer and Rich, 1967; Saenger, 1984). However, any such steric repulsion may be counteracted in the Polι active site cleft by favorable van der Waals contacts between the C5 substituent and Leu78 emanating from the fingers domain. Interestingly, dGTP and dATP insert differently opposite template U/T, namely dGTP in *cis* and dATP in *trans*. However, the incorporation of A or G onto the primer terminus, although highly inefficient, can only occur in the *cis* conformation where the putative 3'OH at the primer terminus is <4Å from the dNTP α-phosphate. We postulate that dATP and dGTP alternate between *cis* and *trans* conformations opposite template T, and that dGTP is (on balance) favored in the *cis* conformation by a hydrogen bond between its N2 amino group and Gln59 of Polι. In all, the structures offer a plausible basis for the inefficiency of nucleotide incorporation opposite template T; wherein, dATP and dGTP interconvert between distorted W-C base-pairing in *cis* and catalytically incompatible base pairing in *trans*. We also show that a hydrogen bond between Gln59 and the N2 amino group of dGTP contributes positively to G incorporation opposite template, whereby dITP (lacking an N2 amino group) is incorporated at ~10-fold lower catalytic efficiency than dGTP and which could account for the preferential incorporation of G over an A opposite template T.

An interesting question is why dATP or dGTP would flip over to the *trans* conformation. We believe that the answer lies in the same structural feature of Polι that make it conducive to Hoogsteen base pairing opposite a template purine, namely a constricted active site that reduces the C1'-C1' distance across the nascent base pair from ~10.5Å in most DNA polymerases to <9Å in Polι (Nair et al., 2005; Nair et al., 2006a; Nair et al., 2006b; Nair et al., 2009; Nair et al., 2004). The template purine sugar is entrenched in a cavity lined by residues from the fingers domain, including the side chain of Leu62 and the aliphatic portions of Gln59 and Lys60, while on the other side of the active site the dNTP sugar is fixed by packing against the aromatic ring of Tyr39, as well as by a hydrogen bond between its 3'OH and the main chain amide of the tyrosine. Template A or G is driven to the *syn* conformation by this "narrowing" of the distance across the incipient base pair in the Polι active site cleft (Nair et al., 2006b). In contrast, a pyrimidine would not free up as much "space" as a purine by rotating to the *syn* conformation due to its smaller size and more isotropic shape. Also, a pyrimidine in the *syn* conformation does not offer the same hydrogen bonding opportunities as a purine in the *syn* conformation, and, in the case of T

the C5 methyl group can sterically overlap with incoming dATP or dGTP. It is not surprising therefore to see BrU in the *anti* conformation when paired with dATP or dGTP, and the "narrowness" of the Polι active site cleft appears to be managed in two ways. First, distorted W-C pairing in *cis* where the bases are somewhat staggered with respect to each other and the C1'-C1' is ~9.6Å and, second, where the incoming dNTP flips over to a *trans* orientation and thereby effectively "removes" the sugar from the constraint of packing against aromatic ring of Tyr39. Interestingly, although *trans* or reverse base pairing is more common in RNA than DNA structures (Fortsch et al., 1996; Lee and Gutell, 2004; Leontis et al., 2002), it has also been observed in a G:T mismatch in the active site of Dpo4 (Trincao et al., 2004), an archaeal Y-family DNA polymerase. In all, the structures we present here complement earlier Polι structures with template purines and provide a basis by which Polι inserts (albeit, highly inefficiently) dATP and dGTP opposite T. Importantly, almost all of the biochemical properties of Polι appear to stem from a constricted active site cleft that permits the bypass of minor-groove purine adducts such as 1, N6-ethenodeoxyadenosine through Hoogsteen base-pairing (Nair et al., 2006a), while at the same time hindering the ability of Polι to insert a nucleotide opposite template pyrimidines.

Experimental Procedures

Crystallization

The GST-Polι (residues 1-420) fusion protein was expressed and purified as described previously (Johnson et al., 2000). A self-complementary 18-mer oligonucleotide was synthesized containing dideoxycytosine at its 3' ends (5'-TCT-BrU-GGGTCCTAGGACCC^{dd}-3', BrU = 5-bromo-deoxyuridine). The oligonucleotide was purified by reverse phase HPLC (on a C18 column), desalted, and lyophilized. Prior to crystallization, the oligonucleotide was annealed with itself to give a "double-ended" template-primer with two replicative ends. For crystallization of the Polι$_{U.dGTP}$ ternary complex, Polι and DNA were mixed in the ratio of 1:1.2, followed by the addition of dGTP and $MgCl_2$ to final concentrations of 20 mM and 10 mM respectively. For the Polι$_U$ binary complex, only protein and the corresponding DNA were mixed together. The ternary and binary complexes were crystallized from solutions containing 10-15 % PEG 5000 MME and 0.2 –0.4 M $(NH_4)_2SO4$ in 0.1 M MES buffer (pH=6.5). Crystals belong to space group $P6_522$ with cell dimensions of a = 98Å, b = 98Å, c = 203Å and α=β=90°, γ=120°. For data collection, the crystals were cryoprotected by soaks for 5 minutes in mother liquor solutions containing 5%, 10% and 15% glycerol, respectively, and then flash frozen in liquid nitrogen.

Structure Determination and Refinement

X-ray data on cryocooled crystals were measured at Advanced Photon Source (APS, beamline 17-ID) of Argonne National Laboratory. Single wavelength anomalous diffraction data on the binary and ternary crystals were collected at a wavelength of 0.920Å corresponding to the peak of the Br *K*-edge absorption profile. Data sets were indexed and integrated using DENZO and reduced using SCALEPACK (Otwinowski and Minor, 1997). The positions of the bromine atoms belonging to 5-bromouracil of the templating base were determined from anomalous difference Fourier maps and helped establish the orientation of the templating base in all three structures. The Polι$_U$, Polι$_{U.dATP}$, and Polι$_{U.dGTP}$ structures were solved by molecular replacement (MR), using the earlier Polι$_{G.dCTP}$ complex as a search model (with dCTP omitted) (Nair et al., 2005). The program AmoRe (Navaza, 1994) gave a unique MR solution in each case. The first round of refinement and map calculation was carried out without the template and the 5' unpaired nucleotides. The electron density maps showed unambiguous densities for the template BrU and the 5' nucleotide, which were then included in the model for subsequent refinement. Iterative rounds of refinement and water picking were performed with CNS (Brunger et al., 1998) and model building with

program O (Jones et al., 1991). All models have good stereochemistry, as shown by PROCHECK (Laskowski et al., 1993) with > 83 % of the residues in the most favored regions of the Ramachandran plot and ≤ 0.6 % in the disallowed regions. Figures were prepared using PyMol (Delano, 2002).

Steady State Kinetic Analyses

The DNA substrate used contained a 32 nt oligonucleotide primer (5'-GTTTTCCCAG TCACGACGATGCTCCGGTAC-3') annealed to a 52 nt template (5'-TTCGTATAATGCCTACACTTGAGTACCGGAGCATCGTCGT GACTGGGAAAAC-3'). The standard DNA polymerase reaction (5μl) contained 25 mM Tris-HCl (pH-7.5), 5 mM MgCl2, 1 mM dithiothreitol, 100 μg/ml BSA, 10% glycerol, various concentrations of dGTP or dITP, 10 nM DNA substrate, and 0.5 nM Polι. All reactions were carried out for 5 min at 37°C. Reaction products were resolved on 13% polyacrylamide gels containing 8M urea. The band intensities of substrate and products of deoxynucleotide incorporation reactions were quantitated by using a PhosphorImager and ImageQuant software (Molecular Dynamics). The observed rate of deoxynucleotide incorporation, V_{obs}, was determined by dividing the amount of product formed by the time of reaction protein concentration used. The V_{obs} was then plotted as a function of deoxynucleotide concentration and the data fitted to Michaelis-Menten equation describing a hyperbola Vobs=(kcat[Enz] × [dNTP]/km+ [dNTP].

Acknowledgments

We thank the staff at the Advanced Photon Source (beamline 17-ID) for facilitating X-ray data collection. We thank Anshu Bhatnagar for contributing to kinetic studies. This work was supported by grant CA115856 from the U. S. National Institutes of Health.

References

Brown T, Kneale G, Hunter WN, Kennard O. Structural characterisation of the bromouracil.guanine base pair mismatch in a Z-DNA fragment. Nucleic Acids Res 1986;14:1801–1809. [PubMed: 3951996]

Brunger AT, Adams PD, Clore GM, Delano WL, Gros P, Grosse-Kunstleve R, Jiang W, Kuszewski J, Nilges M, Pannu NS, et al. Crystallography & NMR system: A software suite for macromolecular structure determination. Acta Cryst 1998;D54:905.

Danilov VI, van Mourik T, Kurita N, Wakabayashi H, Tsukamoto T, Hovorun DM. On the mechanism of the mutagenic action of 5-bromouracil: a DFT study of uracil and 5-bromouracil in a water cluster. J Phys Chem A 2009;113:2233–2235. [PubMed: 19216504]

Delano, WL. The PyMol Molecular Graphics System. Delano Scientific LLC; San Carlos, USA: 2002.

Doublie S, Sawaya MR, Ellenberger T. An open and closed case for all polymerases. Structure Fold Des 1999;7:R31–35. [PubMed: 10368292]

Fortsch I, Fritzsche H, Birch-Hirschfeld E, Evertsz E, Klement R, Jovin TM, Zimmer C. Parallel-stranded duplex DNA containing dA.dU base pairs. Biopolymers 1996;38:209–220. [PubMed: 8589254]

Haracska L, Johnson RE, Unk I, Phillips BB, Hurwitz J, Prakash L, Prakash S. Targeting of human DNA polymerase iota to the replication machinery via interaction with PCNA. Proc Natl Acad Sci U S A 2001;98:14256–14261. [PubMed: 11724965]

Haschemeyer AE, Rich A. Nucleoside conformations: an analysis of steric barriers to rotation about the glycosidic bond. J Mol Biol 1967;27:369–384. [PubMed: 6048986]

Johnson RE, Washington MT, Haracska L, Prakash S, Prakash L. Eukaryotic polymerases iota and zeta act sequentially to bypass DNA lesions. Nature 2000;406:1015–1019. [PubMed: 10984059]

Jones AT, Zou JY, Cowan SW, Kjeldgaard M. Improved methods for building protein models in electron density maps and the location of errors in these models. Acta Cryst 1991;A47:110–119.

Laskowski RA, MacArthur MW, Moss DS, Thornton JM. PROCHECK: a program to check the stereochemical quality of protein structures. J Appl Cryst 1993;A47:110–119.

Lawley PD, Brookes P. Ionization of DNA bases or base analogues as a possible explanation of mutagenesis, with special reference to 5-bromodeoxyuridine. J Mol Biol 1962;4:216–219. [PubMed: 14462975]

Lee JC, Gutell RR. Diversity of base-pair conformations and their occurrence in rRNA structure and RNA structural motifs. J Mol Biol 2004;344:1225–1249. [PubMed: 15561141]

Leontis NB, Stombaugh J, Westhof E. The non-Watson-Crick base pairs and their associated isostericity matrices. Nucleic Acids Res 2002;30:3497–3531. [PubMed: 12177293]

Nair DT, Johnson RE, Prakash L, Prakash S, Aggarwal AK. Human DNA Polymerase iota Incorporates dCTP Opposite Template G via a G.C+ Hoogsteen Base Pair. Structure (Camb) 2005;13:1569–1577. [PubMed: 16216587]

Nair DT, Johnson RE, Prakash L, Prakash S, Aggarwal AK. Hoogsteen base pair formation promotes synthesis opposite the 1,N6-ethenodeoxyadenosine lesion by human DNA polymerase iota. Nat Struct Mol Biol 2006a;13:619–625. [PubMed: 16819516]

Nair DT, Johnson RE, Prakash L, Prakash S, Aggarwal AK. An incoming nucleotide imposes an anti to syn conformational change on the templating purine in the human DNA polymerase-iota active site. Structure 2006b;14:749–755. [PubMed: 16615915]

Nair DT, Johnson RE, Prakash L, Prakash S, Aggarwal AK. DNA synthesis across an abasic lesion by human DNA polymerase iota. Structure. 2009 in press.

Nair DT, Johnson RE, Prakash S, Prakash L, Aggarwal AK. Replication by human DNA polymerase-iota occurs by Hoogsteen base-pairing. Nature 2004;430:377–380. [PubMed: 15254543]

Navaza J. AMoRe: an automated package for molecular replacement. Acta Cryst 1994;50:157–163.

Otwinowski Z, Minor W. Processing of X-ray diffraction data collected in oscillation mode. Methods Enzymol 1997;276:307–326.

Prakash S, Johnson RE, Prakash L. Eukaryotic Translesion Synthesis DNA Polymerases: Specificity of Structure and Function. Annu Rev Biochem 2005;74:317–353. [PubMed: 15952890]

Rothwell PJ, Waksman G. Structure and mechanism of DNA polymerases. Adv Protein Chem 2005;71:401–440. [PubMed: 16230118]

Saenger W. Principles of nucleic acid structure (New York, Springer-Verlag). 1984

Sowers LC, Goodman MF, Eritja R, Kaplan B, Fazakerley GV. Ionized and wobble base-pairing for bromouracil-guanine in equilibrium under physiological conditions. A nuclear magnetic resonance study on an oligonucleotide containing a bromouracil-guanine base-pair as a function of pH. J Mol Biol 1989;205:437–447. [PubMed: 2538629]

Sowers LC, Shaw BR, Veigl ML, Sedwick WD. DNA base modification: ionized base pairs and mutagenesis. Mutat Res 1987;177:201–218. [PubMed: 3561423]

Tissier A, McDonald JP, Frank EG, Woodgate R. poliota, a remarkably error-prone human DNA polymerase. Genes Dev 2000;14:1642–1650. [PubMed: 10887158]

Topal MD, Fresco JR. Complementary base pairing and the origin of substitution mutations. Nature 1976;263:285–289. [PubMed: 958482]

Trincao J, Johnson RE, Wolfle WT, Escalante CR, Prakash S, Prakash L, Aggarwal AK. Dpo4 is hindered in extending a G.T mismatch by a reverse wobble. Nat Struct Mol Biol 2004;11:457–462. [PubMed: 15077104]

Washington MT, Johnson RE, Prakash L, Prakash S. Human DNA polymerase iota utilizes different nucleotide incorporation mechanisms dependent upon the template base. Mol Cell Biol 2004;24:936–943. [PubMed: 14701763]

Watson JD, Crick FH. Genetical implications of the structure of deoxyribonucleic acid. Nature 1953;171:964–967. [PubMed: 13063483]

Zhang Y, Yuan F, Wu X, Wang Z. Preferential incorporation of G opposite template T by the low-fidelity human DNA polymerase iota. Mol Cell Biol 2000;20:7099–7108. [PubMed: 10982826]

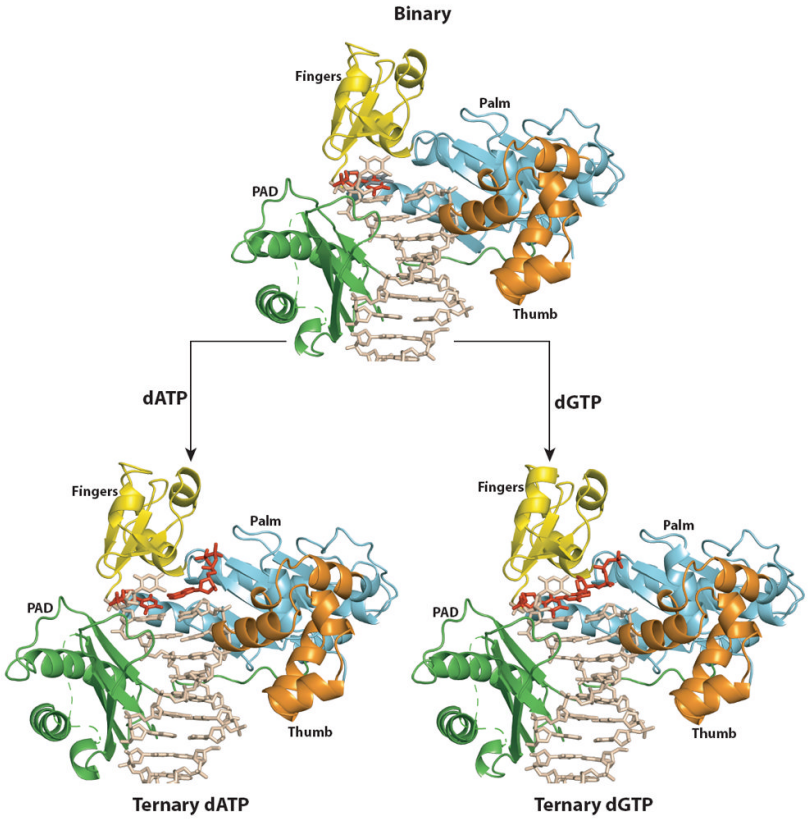

Figure 1. Polι binary and ternary complexes

Overall structures of $Pol\iota_{U}$ (top), $Pol\iota_{U.dATP}$ (bottom left) and $Pol\iota_{U.dGTP}$ (bottom right). Palm, fingers, thumb, and PAD domains are shown in cyan, yellow, orange, and green respectively. DNA is shown in tan; the incoming nucleotide and the template U in *anti* conformation are shown in red. The *syn* conformation of templating U in the binary structure is shown in gray and has been omitted from the ternary structures for clarity.

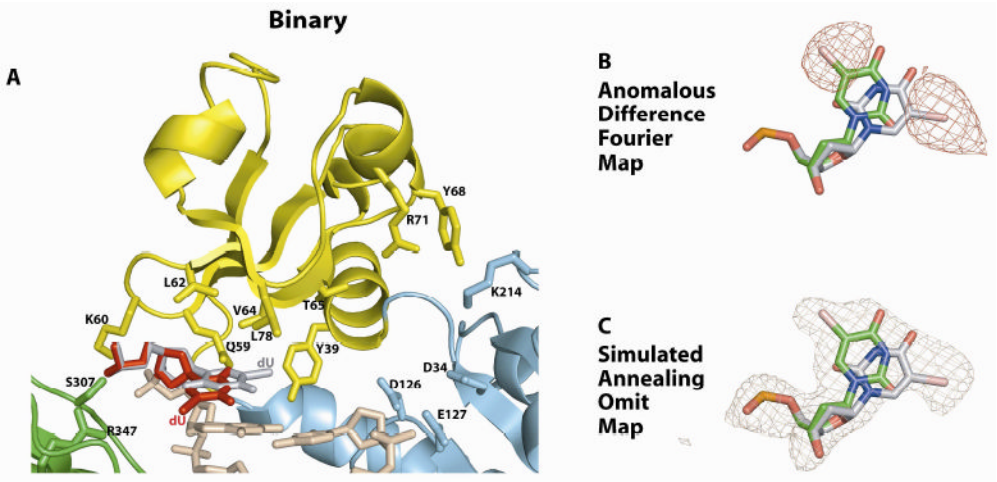

Figure 2. Active site in the Polι_U binary complex

(A) Close-up view of the of Polι_U active site region. The catalytic residues (D34, D126, and E127), the residues apposed to the template U (Q59, K60, L62, V64, L78, S307, and R347) and some other residues near the active site (Y39, T65, Y68, R71, and K214) are highlighted and labeled. The *anti* conformation of template is shown in red and the *syn* conformation in gray. (B) Anomalous difference Fourier map (contoured at 3σ) showing the two positions of the C5 Br atom of the templating base. Based on the map the templating base was modeled in both *anti* and *syn* conformations. (C) Simulated annealing F_o-F_c omit map (contoured at 3σ) with the atoms of the templating base of Polι_U omitted.

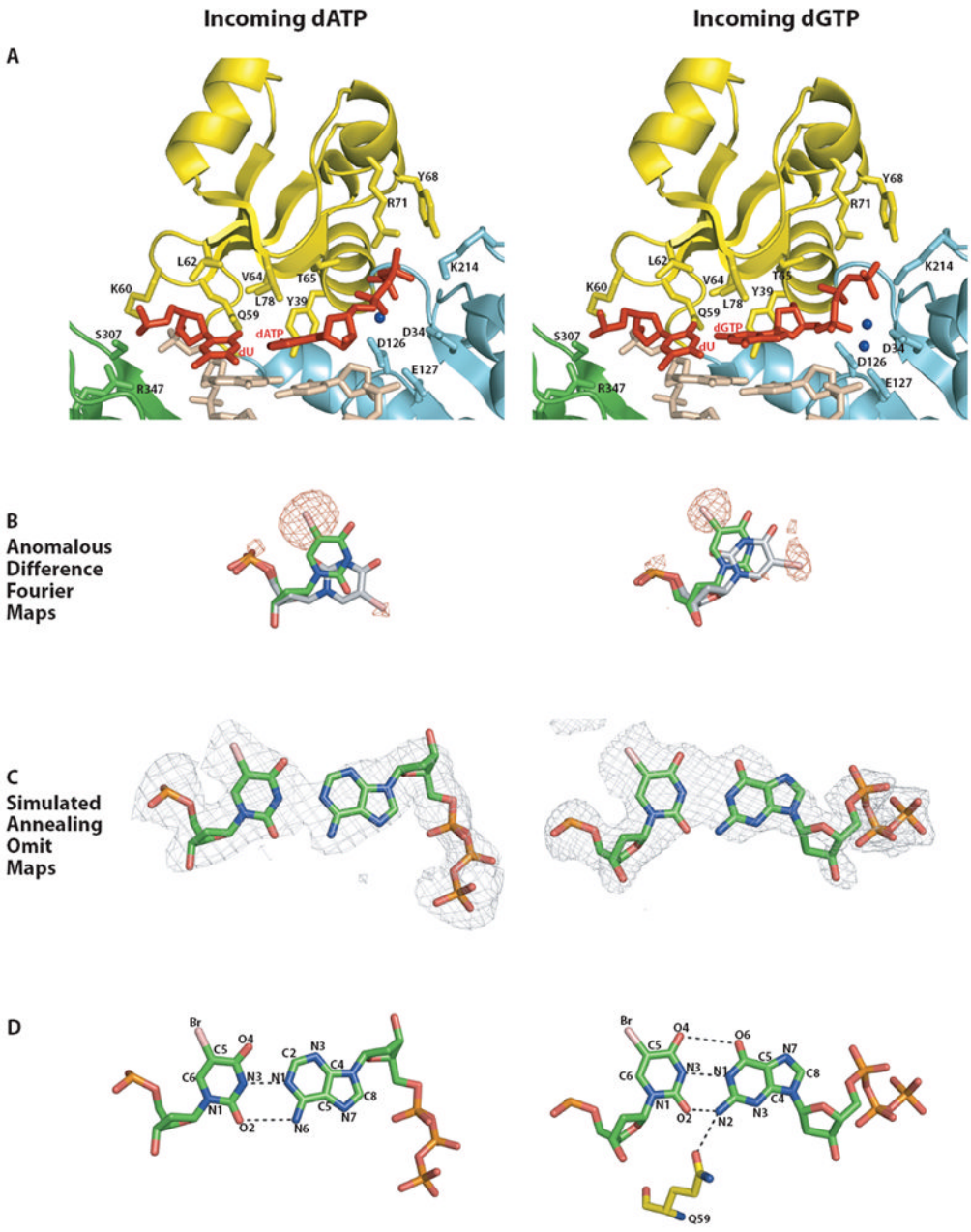

Figure 3. Comparison of the Polι active site in Polι$_{U.dATP}$ and hPolι$_{U.dGTP}$ ternary complexes

(A) Close-up views of the active site regions in Polι$_{U.dATP}$ (left) and Polι$_{U.dGTP}$ (right). Coloring scheme is same as for Figure 1. Putative magnesium ions are shown as blue spheres. The catalytic residues (D34, D126, and E127), residues apposed close to the template base (Q59, K60, L62, V64, L78, S307, and R347), and those near the incoming nucleotide (Y39, T65, Y68, R71, and K214) are highlighted and labeled. The *anti* conformation of templating U and the incoming nucleotide are shown in red. The minor *syn* conformation of the templating base in both the structures has been omitted for clarity. (B) Anomalous difference Fourier maps (contoured at 3σ) showing the position of the C5 Br atoms in the templating base of Polι$_{U.dATP}$ (left) and Polι$_{U.dGTP}$ (right). Note that the density corresponding to the position of the bromine atoms in the *anti* conformation of the template is stronger than that for the *syn* conformation in both ternary complexes. (C) Simulated

annealing F_o-F_c omit maps (contoured at 3σ) around the templating base and the incoming nucleotide in the Polι$_{U.dATP}$ (left) and Polι$_{U.dGTP}$ (right) structures. The template U and incoming nucleotide are in *trans* in the Polι$_{U.dATP}$ complex (left), and in *cis* in the Polι$_{U.dGTP}$ complex (right). (D) U.dATP (left) versus U.dGTP (right) base pairing in the active site of Polι ternary complexes. *trans* orientation coupled with *anti* conformation of U and dATP results in a non-canonical Watson-Crick pair in the active site of Polι$_{U.dATP}$ (left). In Polι$_{U.dGTP}$ (right), incoming dGTP inserts in *cis*, and its N2 amino group forms a hydrogen bond with Gln59 emanating from the fingers domain.

Table 1

Data Collection and Refinement Statistics

Data Collection	**Poli$_U$**	**Poli$_{U.dATP}$**	**Poli$_{U.dGTP}$**
Resolution (Å)	2.3	2.85	2.2
No. of Measured	371962	198630	429934
No. of Unique	26617	14231	30091
Data Coverage (%)	99.7(97.2)	100(100)	99.9(100.0)
R_{merge} (%)[a, b]	6.8(36.1)	9.4(38.0)	8.6 (43.3)
I/σ	44.0(6.0)	31.3 (6.1)	31.4 (5.9)
Refinement Statistics			
Resolution Range	50-2.3	50-2.85	50-2.2
Reflections	25488	13690	28795
R_{cryst} (%)[c]	25.2	24.1	25.4
R_{free} (%)[d]	28.0	28.2	27.0
Non-hydrogen atoms			
Protein	2872	2877	2877
DNA	320	320	320
Incoming NTP		30	31
Mg^{2+} ion		1	2
Water	237	156	272
B factors (Å^2)			
Protein	52.9	52.4	51.5
DNA	54.1	44.1	50.1
Incoming NTP		76.2	50.9
Mg^{2+} ion		57.2	61.4
Water	42.1	38.9	45.4
Rms deviations			
Bonds (Å)	0.006	0.007	0.006
Angles (°)	1.3	1.3	1.2
Ramachandran Plot Quality			
Most favored (%)	86.4	83.8	84.6
Generously allowed	13.3	15.6	15.1
Disallowed (%)	0.3	0.6	0.3

[a] Values for outermost shells are given in parentheses

[b] Rmerge =Σ|I-<I>|/ΣI, where I is the integrated intensity of a given reflection.

[c] Rcryst = $\Sigma||F_{observed}| - |F_{calculated}||/\Sigma|F_{observed}|$

[d] For Rfree calculations ~ 8% of data excluded from refinement was used for the Poli$_U$, Poli$_{U.dATP}$, and Poli$_{U.dGTP}$ complexes.

Table 2

Catalytic efficiency of dGTP *vs*. dITP incorporation opposite template T by Polι

Incoming nucleotide	k_{cat} (min^{-1})	K_m (μM)	k_{cat}/K_m	Efficiency relative to dGTP insertion
dGTP	2.97±0.07	29.8 ±1.74	0.10	-
dITP	1.36±0.03	144.3±13.0	0.01	0.10 (10x↓)

The data represent an average of three experiments